Radiative decay rates of metastable Ar III and Cu II ions

M. H. Prior
University of California, Lawrence Berkeley Laboratory, Berkeley, California 94720
(Received 13 July 1984)

Magnetic dipole ($M1$) and electric quadrupole ($E2$) lines have been observed from trapped metastable Ar III and Cu II ions. The decay of these lines following excitation has yielded the lifetimes (or total radiative decay rates) for the upper levels. The lines observed are, from Ar III, the $M1$ transition at 3109 Å from $^1S_0$ to $^3P_1$ in the ground state $3p^4$ configuration, and from Cu II, the $E2$ lines at 4377 and 3807 Å from $3d^9 4s\ ^1D_2$ and $^3D_2$ to the ground state $3d^{10}\ ^1S_0$. The results for the total radiative rates are $\gamma(^1S_0)=9.2\pm2.3$ sec^{-1} for Ar III and $\gamma(^3D_2)=0.14\pm0.28$ sec^{-1} and $\gamma(^1D_2)=1.95\pm0.24$ sec^{-1} for Cu II. These results are compared to existing theoretical values.

I. INTRODUCTION

The measurement of the radiative lifetimes of metastable ions is an area of study which has remained largely untouched until recent times. This is in spite of the fact that study of forbidden radiation from metastable atomic systems has a long history, extending from the early observations of astrophysical sources (e.g., the nebular lines[1]) to the present-day diagnostic studies of tokamak reactor plasmas.[2] The laboratory measurement of metastable ion radiative lifetimes has utilized principally two techniques, namely decay following beam-foil excitation of fast ions or observation of emission from pulse-excited trapped ions. The beam-foil approach applies well to highly charged, short-lived metastable states, e.g., H-like $2s$ Ar XVIII, whereas the ion-trap methods have been applied so far to singly and doubly charged ions with lifetimes up to about 1 min.

In this work we report studies of metastable Cu II and Ar III ions (members of the Ni and S isoelectronic sequences) in which the electrostatic ion trap is used for the first time in lifetime measurements. We have observed electric quadrupole ($E2$) lines in emission from Cu II ions in the $3d^9 4s\ ^1D_2$ and $^3D_2$ states, and the 3109-Å magnetic dipole ($M1$) line emitted by Ar III ions in the $3p^4\ ^1S_0$ state. To our knowledge these are the first laboratory observations of these lines, although the Ar III line and the 3807-Å line from $^1D_2$ Cu II have been seen in emission from astrophysical sources (for Ar III see Ref. 1, for Cu II see Ref. 3). In more highly ionized members of the Ni sequence, Cocke and collaborators[4] have observed the $E2$ lines and measured the lifetimes of the $^1D_2$ and $^3D_2$ states in I XXVI using the beam-foil technique, and Klapisch *et al.*[5] have observed both $E2$ lines from Mo XV excited in the tokamak at Fontenay-aux-Roses (TFR). The $M1$ line from $3p^4\ ^1S_0$ has been observed[6] from Cr X, Fe XII, and Ni XIII in the solar corona.

II. EXPERIMENTAL METHOD

The basic method used in these studies was the same for both ions, although there are important differences which will be discussed. In each case, the ions were stored after excitation in an electrostatic trap of the type first described by Kingdon[7] and recently used[8] for low-energy-electron capture studies. A fraction of the forbidden radiation emitted by the metastable ions during the storage time entered a small spectrometer ($\frac{1}{4}$-m Jarrell Ash 82-415) and was detected by a photomultiplier mounted at the exit slit. Scanning the spectrometer in synchronism with the channel advance of a multichannel scalar (MCS) produced records of the forbidden line spectra. To record a decay curve, the spectrometer was set to the peak of the desired line, and counts were stored in the MCS with the channel advance derived from a clock pulse with a frequency which could be chosen to suit the particular case under study. In both studies a quadrupole mass analyzer (QMA) was mounted near the ion trap and was used to analyze the mass to charge spectrum of ions ejected radially from the trap by a positive potential applied to the central wire. By dumping the trap at successively delayed times following the fill period, decay curves of the total ion population (including all excited states) could be obtained.

The ion traps used for the two ions differed but not in any essential way. The major difference was in the methods of excitation and ionization. In the case of Ar III, the ions were made by electron impact upon Ar gas at low pressure [$(1-10)\times10^{-7}$ Torr] which filled the experimental chamber. The electron beam entered the ion trap parallel to the trap central wire. Care was taken to reduce the flux of photons emitted from the electron cathode and scattered into the spectrometer entrance slit. This was done by using a low-temperature dispenser cathode and by masking and baffling the electron gun assembly. The electron current was on-off modulated by switching the cathode potential. Figure 1 shows the experimental arrangement used in the Ar III measurements.

The Cu II ions were made by a vacuum spark technique, with the spark located external to the ion trap. The arrangement is shown in Fig. 2. A vacuum breakdown is initiated by a spark-gap-triggered transfer of positive charge (at about 20 kV potential) from a 500-pF capacitor to a tantalum wire (0.020 in. diam) located near a small piece of copper sheet. The copper sample is held on the end of a vacuum manipulator; this allows adjustment of

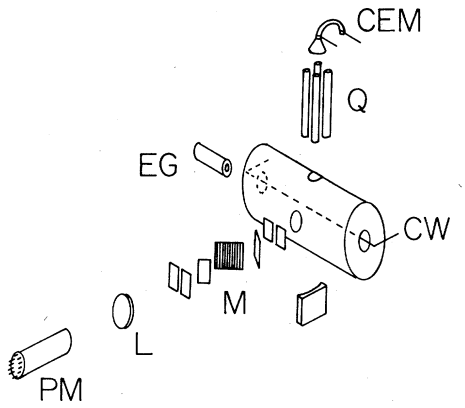

FIG. 1. Experimental arrangement for the Ar III studies. CW, ion-trap central wire; EG, electron gun; Q, quadrupole mass analyzer (QMA); CEM, channel electron multiplier detector for the analyzer; M, $\frac{1}{4}$-m spectrometer; L, lens to focus the exit slit of M onto photomultiplier, PM.

the electrode gap and the place on the Cu sheet where the spark occurs. The brief (≈ 10 μsec) discharge produces a plasma plume which expands outward with ion energies of a few hundred eV. Many of the fast ions and atoms in the plume strike the surrounding walls in the chamber sidearm containing the spark electrodes, a smaller fraction proceed across the main chamber, passing through the ion trap. After the spark discharge, one finds that the trap is filled with ions derived from the plume and its interaction with the chamber walls. These ions can then be held without loss for many seconds, the time determined largely by collisions with the residual gas in the vacuum chamber.

Analysis of the stored ions was made with a QMA used to sample ions ejected from the trap by raising the wire potential to ground. This analysis showed that, in addition to Cu II ions, there were Fe, Cr, and Ni ions created by sputtering from the chamber walls (no Ta ions were seen). These were eliminated by surrounding the region of the spark with a copper sheet liner so that the sputtered material would add to the population of Cu ions in the

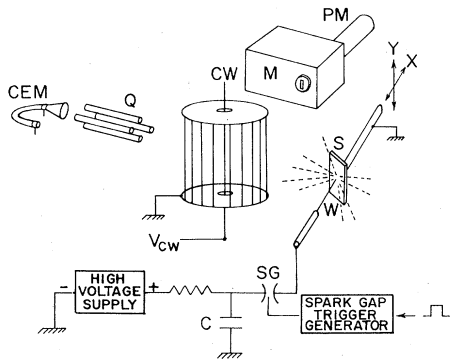

FIG. 2. Experimental arrangement for the Cu II studies. Much of the nomenclature is as in Fig. 1. Spark gap SG transfers charge from C (500 pF) to a 0.020-in. Ta wire, W, located near the Cu sample S. A manipulator allows motion of the sample in the X and Y directions. The potential V_{cw} ranged from -200 to -1000 V.

trap. (There are of course many metastable levels in the iron group ions and these will undoubtedly be studied in future work.) There remained a small trace of H_2O fragment ions presumably made by impact upon the residual water vapor in the chamber or perhaps also liberated from the solid material surrounding the spark. Thus a nearly pure sample of Cu II ions was obtained for storage, a fraction of which came from the spark discharge itself, and a nonnegligible remainder which came from sputtering of the copper liner. These observations are similar to those of Cody *et al.*[9] and Knight[10] of ions produced and trapped from pulsed laser interaction with metal targets.

The mechanism for injecting ions for storage from an external transient source such as described here, relies upon the shielding by the advancing charge cloud so that the ions on the interior or trailing portions of the cloud enter the trap volume without sensing the negative trap potential. As the cloud expands further, the shielding switches off and some ions are captured. In addition, one can expect ion-ion and ion-atom collisions to make some contribution to filling the trap, since both momentum exchange and charge transfer can lead to one partner bound in the trap. In the case of momentum exchange a simple mechanical analogy would be filling a bucket with ping-pong balls by tossing them from some distance. One at a time, they each bounce out, but thrown in handfulls, often some remain.

The spark was triggered by the trap timing system and could be run at a repetition rate as high as about 10 Hz. Since, as one might expect, the sparks showed considerable variation in the resulting ion population captured by the trap, often a series of sparks (typically four) were fired before initiating study of the forbidden radiation; this tended to average the shot-to-shot variation.

III. DATA AND RESULTS

A. Ar III

Figure 3 shows the energy-level scheme for the Ar III $3p^4$ ground configuration. The $^1S_0$ level is predicted[11,12] to decay principally by the 3109-Å $M1$ ($\approx 60\%$) and 5192-Å $E2$ ($\approx 40\%$) branches. Figure 4 is a survey scan with the spectrometer showing the 3109-Å $M1$ line with about a one-to-one signal-to-background ratio with no

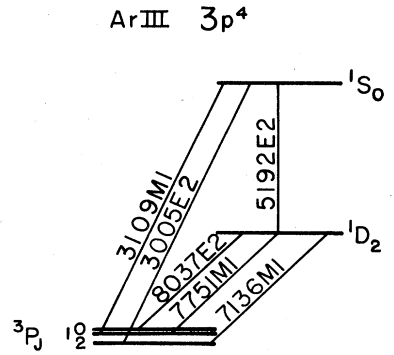

FIG. 3. Energy-level diagram for the Ar III $3p^4$ ground configuration showing the $M1$ and $E2$ transitions.

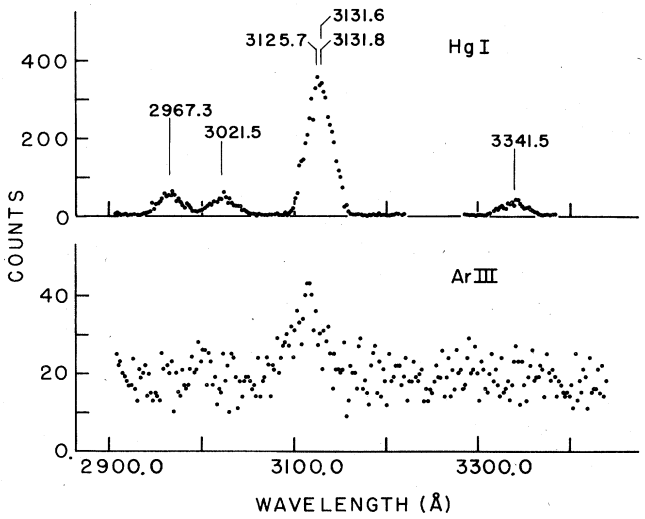

FIG. 4. Spectrometer scan showing the Ar III 3109-Å $M1$ line and a Hg I reference spectrum.

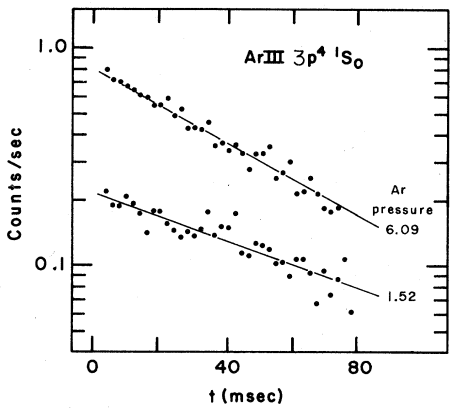

FIG. 5. Decay curves obtained at two Ar pressures (in units of 10^{-7} Torr) by monitoring the 3109-Å $M1$ line vs time after filling the ion trap.

comparable features in the wavelength range 2900—3370 Å. The upper portion of the figure shows a spectrum obtained from a Hg calibration lamp. Because the Ar III emission is weak, the spectrometer slits were wide, resulting in a resolution of about 20 Å. The Ar III spectrum was accumulated in approximately 3 h; the signal rate at the peak is about 0.6 sec^{-1} above the background. During this collection period, the trap cycle consisted of a 3.5-msec electron current pulse at an energy of 150 eV, followed by a 21-msec storage time during which counts from the cooled photomultiplier (EMI 9789) were accumulated, followed by a brief dump pulse to the trap wire (in which it was raised from -9.0 to $+13.0$ V) which emptied the trap. Attempts to observe the 5192-Å $E2$ branch were unsuccessful because of the increased background intensity from the electron gun cathode in this wavelength region. The background rate near the 3109-Å line (Fig. 4) arises almost entirely from the dark rate of the cooled photomultiplier.

In Fig. 5 are shown two decay curves taken with the spectrometer set to the 3109-Å peak. The data have had an experimentally determined background subtracted. This was done by dumping the trap some time before reaching the end of each scan of the MCS, so that the final channels contained counts received with no ions in the trap. This trap-empty count was then subtracted from each channel to yield the decay curves. The two curves shown were taken with different Ar gas pressures in the chamber as noted in the figure in units of 10^{-7} Torr (as read by a nude ionization gauge). Decay curves were taken at four different Ar pressures, namely 1.5×10^{-7}, 3.7×10^{-7}, 6.1×10^{-7}, and 8.6×10^{-7} Torr (indicated ionization gauge readings) and the least-squares-fitted decay rates were 12.4, 14.2, 18.2, and 19.6 sec^{-1}, respectively. The decay rate at zero Ar pressure obtained from a fit to the rate versus pressure data yielded $\gamma'=10.7\pm0.8$ sec^{-1}.

In order to make some estimate of the size of the decay rate associated with collisions with the residual gas in the vacuum chamber, we also measured decay curves for the total number of Ar III ions at various pressures. This was done by accumulating the Ar III signal from the QMA versus storage time. These ion decay curves appeared to be single exponentials, but with decay constants whose dependence upon Ar pressure was approximately 60% larger than that of the $^1S_0$ emission decay. If one takes the Ar pressure to be given by the indicated reading corrected by the factor 0.62, then the collision rate constant for the Ar-induced $^1S_0$ decay was measured to be $k_0=(5.5\pm0.8)\times10^{-10}$ $\text{cm}^3\,\text{sec}^{-1}$, whereas that for the total ion population was $k_t=(8.9\pm0.5)\times10^{-10}$ $\text{cm}^3\,\text{sec}^{-1}$. Johnson and Biondi[13] have reported drift-tube mass-spectrometer measurements of thermal-energy (300 K) single-electron charge-transfer rate coefficients for the metastable and ground levels of Ar III ions in collision with Ar and other noble gases. These authors observed a marked variation of the rate constants for the different levels, although their values were at least a factor of 100 smaller than the rates quoted above. In addition, Johnson and Biondi observed that the $^1S_0$ level had the largest rate constant, whereas our observations show a $^1S_0$ loss rate constant smaller than that for the whole ion population. The mean energy of the trapped Ar III ions in our work was about 1.3 eV, which is considerably higher than in the studies of Johnson and Biondi; this may account for the difference in our rate constants. Recently Huber and Kahlert[14] have shown that the Ar III metastable and ground-state levels have significantly different charge capture cross sections in collision with He, Ne, and Kr target atoms at energies of 600 eV. If the ion population is distributed statistically among the ground and metastable levels, then one would expect 6.7% $^1S_0$, 33.3% $^1D_2$, and 60% $^3P_{2,1,0}$. Thus the total ion decay signal should be dominated by the $^1D_2$ and $^3P_{2,1,0}$ states, and could well show a larger collision rate constant than that for $^1S_0$. Of course, state-dependent rate constants for ion loss should manifest themselves as a departure from single-exponential decay in the QMA signal. However, this behavior may not be visible if the difference is only large between $^1S_0$ and the other levels, because of its small fractional population.

The fit to the ion decay rates versus pressure yielded a zero-argon-pressure ion loss rate of 1.5 ± 0.5 sec^{-1}. To

correct γ' for the collisional loss rate of the $^1S_0$ Ar III ions on the residual gas constituents we subtract this value from γ'. We assign a 100% uncertainty to this correction which we add linearly to the statistical error in γ'. Thus our value for the $^1S_0$ total radiative decay rate is $\gamma(^1S_0)=9.2\pm2.3$ sec^{-1}.

B. Cu II

Figure 6 shows a spectral scan of the region from 3500 to ≈4500 Å taken with Cu II ions stored in the trap shown in Fig. 2. The $E2$ lines at 3807 and 4377 Å appear clearly as the only significant features in this region. The wavelength scale was calibrated using a Hg lamp and the resolution of the spectrometer was about 25 Å. These data were collected with the trap wire potential at −1000 V and each channel is the average of the counts received in a 1-sec period following a single spark. After each spark, the spectrometer was advanced and the full scan was repeated 20 times; approximately 1 h was required to collect these data. The background rate between the peaks in Fig. 6 is the dark rate of the (in this case) uncooled photomultiplier.

Figure 7 presents two representative decay curves, one each for the 3807- and 4377-Å lines and the least-squares-fitted curves to the data. Although not shown, data for the slower decaying 4377-Å line were collected for periods extending to 4 or 8 sec, and the fits were made over the whole interval. One can see that the 3807-Å data show clear departure from single-exponential decay at short times ($\lesssim$0.2 sec). The shape of the curve is indicative of a cascade feeding of the upper $^1D_2$ state and the data were fit with two exponentials plus a constant background. Thus there were generally five parameters in the fit to the 3807-Å decay data. The 4377-Å line did not show significant departure from single-exponential decay over the time scale for which data were collected, and its decay was fit by a single exponential plus a constant background (three parameters).

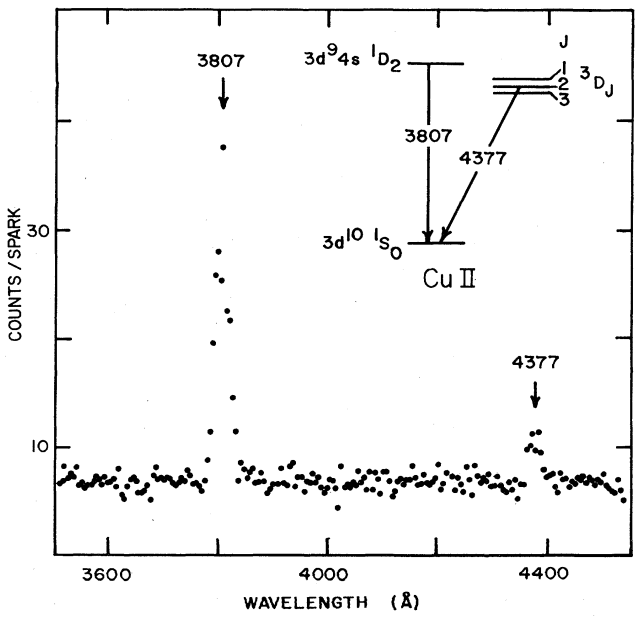

FIG. 6. Spectrometer scan showing the Cu II $E2$ lines studied; the energy-level diagram shows the ground-state and first excited configuration levels.

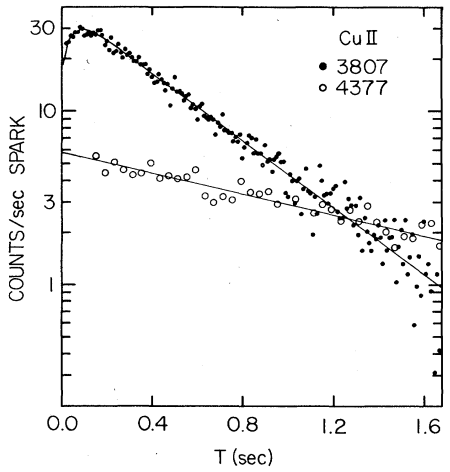

FIG. 7. Decay curves for the 3807- (solid points) and 4377-Å (open circles) Cu II $E2$ lines.

Decay data were collected for both lines at two different residual gas base pressures, namely 1.45×10^{-8} and 0.55×10^{-8} Torr. These were the base pressures without and with, respectively, liquid-nitrogen cooling of a cold trap mounted above the diffusion pump which evacuated the experimental chamber. For the 3807-Å line the mean values from several measurements of the decay rates were 2.27 ± 0.06 and 2.08 ± 0.05 sec^{-1} at the higher and lower pressures, respectively. These rates refer to the longer lifetime component of the two-exponential fit. For the 4377-Å line, the values 0.73 ± 0.12 and 0.37 ± 0.06 sec^{-1} were measured. These values extrapolated to $\gamma'(^1D_2)=1.96\pm0.12$ sec^{-1} and $\gamma'(^3D_2)=0.15\pm0.16$ sec^{-1} at zero residual gas pressure.

The major change in the residual gas composition on cooling the cold trap to 77 K is a reduction of the partial pressures of H_2O, CO_2, and other condensible gases. A study with the quadrupole mass analyzer showed that most of the residual gas in the experimental chamber was composed of species yielding peaks with masses less than 100 amu, the principal peak being $(H_2O)^+$ and its fragment ions and the others probably derived from the diffusion pump fluid (DC 705). Upon cooling the cold trap to 77 K, all of these peaks decreased, with the H_2O peaks dropping somewhat more than those associated with the pump fluid vapor fragments. The fractional decrease in the H_2O peaks was essentially the same as that for the total pressure as read by the nude ionization gauge on the chamber. Thus it seems reasonable to extrapolate the measured decay rates to zero pressure utilizing the ion gauge readings. However, one should keep in mind that the gas composition is changing somewhat as the cold trap is cooled.

We also studied the decay of the total Cu II ion signal at the two residual gas conditions (trap cold and warm) using the QMA set to one of the Cu II isotope peaks. This showed a decay rate of 0.162 ± 0.030 sec^{-1} at a pressure of 0.76×10^{-8} Torr and 0.305 ± 0.060 sec^{-1} at

1.50×10^{-8} Torr. These extrapolate to a rate of 0.013 ± 0.120 sec^{-1} at "zero" pressure. This rate is subtracted from the γ' values and the uncertainties are added linearly to yield our values for the radiative decay rates: $\gamma(^1D_2)=1.95\pm0.24$ sec^{-1} and $\gamma(^3D_2)=0.14\pm0.28$ sec^{-1}.

The fast component of the two-exponential fit to the 3807-Å decay curves had rates of 15.7 ± 3.8 and 23.3 ± 4.8 sec^{-1} at the 1.45×10^{-8} and 0.55×10^{-8} Torr base pressures, respectively. Although these values agree within their uncertainties, the apparent trend with pressure is reverse to that which one would expect for a collision-induced process.

IV. DISCUSSION

The forbidden transition rates for the $3p^4$ Ar III levels (Fig. 3) have been treated theoretically by Czyzak and Krueger[11] (CK) and more recently by Mendoza and Zeippen[12] (MZ). We compare these authors' calculations for the $3p^4$ decay branches together with our measured total radiative rate in Table I. One sees that the two theoretical calculations are in reasonable agreement, differing most (about 20%) in the $E2$ branch to $^1D_2$. Neither of these sets of authors have provided estimates of the uncertainty in their calculations; however, Weise, Smith, and Miles in their critical compilation[15] have suggested an uncertainty of 25% in the values obtained by CK. The work of MZ includes a number of features not treated by CK, such as configuration interaction and relativistic corrections to the $M1$ operator; we expect that their results have a precision at least equivalent to that of CK. One notes, however, the closer agreement of the measured total rate with the CK result; both calculations are in agreement if one assigns 25% uncertainty to each.

Theoretical studies of the forbidden transition probabilities in Cu II have been carried out by Garstang[16] and Beck.[17] Garstang's values for the $E2$ and $M1$ transition probabilities which determine the $3d^94s\ ^1D_2$ and $^3D_2$ total radiative decay rates are shown in Table II together with our measured values. Garstang also calculated $E2$ rates to the ^3D_J levels, but these are all smaller than 2.1×10^{-6} sec^{-1} and hence make insignificant contributions. There is agreement between our measured values and the total decay rates obtained from Garstang's calculations. Beck's treatment is addressed only to the $E2$ transition probability and does not include intermediate coupling; it is, however, an *ab initio* theory and treats many-electron correlation effects. Beck's values for the $E2$ transition rates from $^1D_2$ to $3d^{10}\ ^1S_0$ are 2.33 and 2.21 sec^{-1} using the length and velocity gauge operators, respectively. These are best compared with the sum of Garstang's values for $^1D_2$ and $^3D_2$, i.e., 2.02 sec^{-1}. If we subtract Garstang's $M1$ rates from our measured values and add the results for the two upper levels, we obtain 1.63 ± 0.37 sec^{-1} as an estimate of the pure LS-coupling $E2$ transition rate for $^1D_2-{}^1S_0$. This is in reasonable agreement with Beck's calculations (for which no error estimates were provided).

TABLE I. Ar III $E2$ and $M1$ transition rates (sec^{-1}) from $3p^4\ ^1S_0$ to $^3P_{1,2}$ and $^1D_2$ levels. (CK is Ref. 11 and MZ is Ref. 12.)

Authors	$^3P_1$	$^3P_2$	$^1D_2$	Total
CK	4.02	0.04	3.10	7.16
MZ	3.91	0.04	2.59	6.54
This work				9.2±2.3

Finally, we consider the origin of the apparent two-component nature of the experimental decay curves obtained for the 3807-Å Cu II $E2$ line. Our current data set does not allow us to conclusively determine whether this effect is due to a radiative cascade from a higher-lying metastable level or a collisional transfer from one of the unobserved long-lived $3d^94s\ ^3D_{1,3}$ levels. There are at least two higher-lying long-lived levels in the Cu II structure.[18] One candidate is $3d^84s^2\ ^3F_4$ at 69 704.8 cm^{-1}; the only $E1$ decay path available to this level is to the nearby $3d^94p\ ^3F_3$ state at 68 447.8 cm^{-1}. The small energy separation (1257 cm^{-1}) and the nominal two-electron character of this transition would argue that this transition probability is low. The subsequent decay of the $^3F_3$ state would be rapid and a signature of this process would be radiation at 2150, 2193, and 2371 Å from the branches to the metastable $3d^94s\ ^3D_{3,2}$ and $^1D_2$ levels. All of these lines should show the same apparent decay rate, determined by the rate at which $3d^84s^2\ ^3F_4$ feeds $3d^94p\ ^3F_3$. However, the transition probability[19] for the branch to metastable $^3D_2$ exceeds that to $^1D_2$ by about a factor of 7, which would lead to growth behavior in the 4377-Å $E2$ line decay which was not observed. Another, higher-lying level which must be metastable is $3d^84s4p\ ^5G_6$ near 110 000 cm^{-1}. All levels below this one have $J\leq4$ so that electric dipole decay is strictly forbidden (hyperfine mixing can alter this for some of the F levels, but the statement remains true for the level with maximum $F=I+J$). It is possible that a cascade starting from this level could selectively feed the $3d^9\,4s\ ^1D_2$ level.

Collisional population of $3d^94s\ ^1D_2$ from the metastable ^3D_J levels could also explain the observed apparent two-component decay curve for the Cu II 3807-Å line. This would require collision rate constants near 10^{-7} cm^3 sec^{-1}, however, to reproduce the observed growth rate at the background gas densities ($\approx3\times10^8$ cm^{-3}) in the ion-trap chamber. One would also expect to observe a decrease in the growth rate for data taken at the

TABLE II. Calculated $E2$ and $M1$ transition rates (sec^{-1}) from Ref. 16 for decay branches of Cu II $3d^94s\ ^1D_2$ and $^3D_2$ levels and our measured total rates.

Upper state	$^1S_0$ ($E2$)	$^3D_3$ ($M1$)	$^3D_2$ ($M1$)	$^3D_1$ ($M1$)	Total theor.	Total expt.
$^1D_2$	1.9	0.23	0.18	0.031	2.2	1.95±0.24
$^3D_2$	0.12	0.017			0.14	0.14±0.28

lower residual gas pressure. This is not evident in our data.

Thus at this time we have no satisfactory explanation for the early time behavior of the 3807-Å line decay from the trapped Cu II ions. Further studies should include a search at shorter wavelengths for possible cascade photons from higher-lying states, as well as improved studies of the pressure dependence of the decay rates with emphasis upon obtaining lower base pressures. This would have the benefit of greatly reducing the uncertainty in the 4377-Å measurements where currently the collisional quenching rates are the same size as the radiative decay rate; this leads to a large fractional error in the zero-pressure extrapolated value.

ACKNOWLEDGMENT

This work was supported by the Director, Office of Energy Research, Office of Basic Energy Sciences, Chemical Sciences Division of the U.S. Department of Energy under Contract No. DE-AC03-76SF00098.

[1]I. S. Bowen, Rev. Mod. Phys. **8**, 55 (1936); Astrophys. J. **132**, 1 (1960).

[2]A recent summary of forbidden lines in tokamak plasmas was made by B. C. Fawcett, J. Opt. Soc. Am. **B1**, 195 (1984).

[3]A. D. Thackeray, Mon. Not. R. Astron. Soc. **113**, 211 (1953).

[4]C. L. Cocke, S. L. Varghese, J. A. Bednar, C. P. Bhalla, B. Curnutte, R. Kauffman, R. Randall, P. Richard, C. Woods, and J. H. Scofield, Phys. Rev. A **12**, 2413 (1975).

[5]M. Klapisch, J. L. Schwob, M. Finkenthal, B. S. Fraenkel, S. Egert, A. Bar-Shalom, C. Breton, C. DeMichelis, and M. Mattioli, Phys. Rev. Lett. **41**, 403 (1978).

[6]G. D. Sandlin, G. E. Brueckner, and R. Tousey, Astrophys. J. **214**, 898 (1977).

[7]K. H. Kingdon, Phys. Rev. **21**, 408 (1923).

[8]M. H. Prior, R. Marrus, and C. R. Vane, Phys. Rev. A **28**, 141 (1983).

[9]R. B. Cody, R. C. Burnier, W. D. Reents, T. J. Carlin, D. A. McCrery, R. K. Lengel, and B. S. Frieser, Int. J. Mass Spectrom. Ion Phys. **33**, 37 (1980).

[10]R. D. Knight, Appl. Phys. Lett. **38**, 221 (1981).

[11]S. J. Czyzak and T. K. Krueger, Mon. Not. R. Astron. Soc. **126**, 177 (1963).

[12]C. Mendoza and C. J. Zeippen, Mon. Not. R. Astron. Soc. **202**, 981 (1983).

[13]R. Johnson and M. Biondi, Phys. Rev. A **20**, 87 (1979).

[14]B. A. Huber and H. J. Kahlert, J. Phys. B **16**, 4655 (1983).

[15]W. L. Weise, M. W. Smith, and B. M. Miles, *Atomic Transition Probabilities, Sodium Through Calcium,* Natl. Bur. Stand. (U.S.), Natl. Stand. Ref. Data Ser., No. 22 (U.S. GPO, Washington, D.C., 1969), Vol. II.

[16]R. H. Garstang, J. Res. Nat. Bur. Stand., Sect. A **68**, 61 (1963).

[17]D. R. Beck, Phys. Rev. A **23**, 159 (1981).

[18]C. E. Moore, *Atomic Energy Levels,* Natl. Stand. Ref. Data Ser., No. 35 (U.S. GPO, Washington, D.C., 1970), Vol. II [reissue of NBS Circ. No. 467 (1952)].

[19]A. Kono and S. Hattori, J. Opt. Soc. Am. **72**, 601 (1982).